Nonlinear stress and fluctuation dynamics of sheared disordered wet foam

Ethan Pratt
Department of Physics, California Polytechnic State University, San Luis Obispo, California 93407

Michael Dennin
Department of Physics and Astronomy and Institute for Interfacial and Surface Science, University of California at Irvine, Irvine, California 92697

(Received 7 January 2003; published 9 May 2003)

A sheared wet foam, which stores elastic energy in bubble deformations, relaxes stress through bubble rearrangements. The intermittency of bubble rearrangements in the foam leads to effectively stochastic drops in stress that are followed by periods of elastic increase. We investigate global characteristics of highly disordered foams over three decades of strain rate and almost two decades of system size. We characterize the behavior using a range of measures: average stress, distribution of stress drops, rate of stress drops, and a normalized fluctuation intensity. There is essentially no dependence on system size. As a function of strain rate, there is a change in behavior around shear rates of 0.07 s^{-1}.

DOI: 10.1103/PhysRevE.67.051402 PACS number(s): 83.80.Iz, 82.70.−y

I. INTRODUCTION

One of the potentially exciting features of driven, complex fluids is the possible existence of an ''effective'' temperature [1,2]. Examples of systems for which an effective temperature may prove to be a useful idea include foams, emulsion, granular materials, and colloidal glasses (for example, see Ref. [3], and references therein). Theoretical studies of effective temperatures using the bubble model of foams [1] and the ''standard model'' for a supercooled liquid (a binary Lennard-Jones mixture) [2] provide a strong motivation for experimental studies of effective temperature. Understanding the nature of fluctuations in these systems is a key step toward developing an understanding of any concept of effective temperature. In this paper, we focus on fluctuations in a sheared, two-dimensional foam system: bubble rafts [4,5]. Under shear, an initially jammed foam exhibits an elastic behavior until it reaches the yield strain, followed by intermittent ''stress drops'' as the bubbles undergo nonlinear topological rearrangements (for a review on foams, see Refs. [6–8]). The fluctuations in stress, and other quantities in the system, are reminiscent of thermal fluctuations and motivate definitions of effective temperature. A previous work with bubble rafts characterized the statistical distribution of stress drops for a single system size and a small range of strain rates [5]. The results were in an excellent agreement with simulations of the bubble model [9–11]. In this paper, we will report on results for a greater range of system size and strain rate. Additionally, we will report on a number of measures other than the distribution of stress drops. In addition to providing a starting point for studies of effective temperatures, this work provides detailed tests of competing models of flowing, two-dimensional foams.

There are a number of different models of flowing foam. They all make qualitatively similar predictions regarding the behavior of the stress as a function of strain rate. For small rates of strain, there is an initial elastic region. At a critical value of the stress (yield stress) or strain (yield strain), the foam begins to flow. The flow in this region is intermittent, with periods of increase followed by sudden, irregular stress releases, referred to as stress drops. Where the models differ among themselves is the details of the distribution of stress drops. These differences are the result of different assumptions concerning the source of dissipation and dryness of the foam. As this work focuses on two-dimensional foams, the ''dryness'' is characterized by the area fraction of gas, ϕ. For $\phi=1$, the foam is perfectly dry, and the bubbles are all polygons. For $\phi<0.84$, the foam ''melts'' into a froth of exclusively circular bubbles. Foams near this limit are referred to as ''wet.''

Four main models of a two-dimensional foam are the vertex model [12–14]; the quasistatic model [15,16]; the extended q-Potts model [17]; and the bubble model [9–11]. The vertex model is not particularly relevant to our system, since it models dry foam. The quasistatic model is special because it does not contain any dissipation. It deals with wet foams. The results from this model suggest a power-law distribution for the probability of stress drops of a certain size occurring [15,16]. This result is based mainly on measuring the distribution of $T1$ events. The $T1$ events are nonlinear neighbor switching events between four bubbles. The extended q-Potts model includes dissipation without making any specific assumptions about the dissipation. The work in Ref. [17] focuses on the dry foam limit, but the model can treat wet foams. These simulations suggest that a quasistatic limit does not exist for foam. In other words, as the strain rate is continually decreased, the properties of the flow continue to change. Also, they report a transition, as a function of disorder, from a viscoelastic solid to a viscoelastic fluid. The signature of this change was the fact that sufficiently disordered foams displayed no yield strain. Instead, such foams flowed immediately upon the application of shear. Finally, this work suggests that the distribution of energy drops in sheared foam obeys a power law. However, the distribution of $T1$ events does not. The bubble model is applicable to wet foams, and its main prediction with regard to stress drops is a power-law distribution for small stress drops with an exponential cutoff at larger stress drop magnitudes

[9–11]. In contrast to the q-Potts model, the bubble model does predict a quasistatic limit for flowing foams.

Experiments with foam have yielded various results. Indirect studies of a three-dimensional foam using diffusive wave spectroscopy suggest a cutoff to the nonlinear rearrangements [18]. Studies of $T1$ events using two-dimensional foams agree with these results [19]. These experiments used the gas-liquid coexistence region of Langmuir monolayers to make truly two-dimensional foams. Experiments using quasistatic shear of a single layer of bubbles between glass plates suggest that there may be system-wide events, suggesting a possible power-law behavior [20]. Work with bubble rafts (a single layer of bubbles on the surface of water) showed that the distribution of stress drops for a system of ≈ 900 bubbles exhibited the exponential cutoff predicted by the bubble model [5]. In order to further test the agreement with the bubble model, we have extended the work in Ref. [5] to a wide range of system sizes and strain rates. Furthermore, in addition to reporting on the distribution of stress drops, we also measure the rate of stress drops, the average stress (which gives the viscosity) and the normalized stress fluctuation. We establish that the cutoff in stress drops is not a finite size effect. Also, we show that for this system there is a well-defined quasistatic limit, as predicted by the bubble model. Finally, we will discuss the apparent dependence of some of the properties on system size and strain rate. The rest of the paper is organized as follows. Section II describes the experimental techniques. Section III presents the results. Section IV discusses the results in context of the various models of foams.

II. EXPERIMENTAL DETAILS

A standard bubble raft [4] provides an efficient model system for studying two-dimensional foams. Bubble rafts consist of a layer of bubbles floating on the surface of water. The motion of the bubbles is essentially all in the plane defined by the water surface. However, it should be noted that the system is not an ideal, two-dimensional system, since some motion is possible perpendicular to the surface. However, in all of our experiments, the bubbles were monitored with video cameras, and no motion was observable perpendicular to the water surface. The bubble raft was produced by flowing regulated nitrogen gas through a hypodermic needle into a homogeneous solution of 82.0% by volume glycerine, 14.5% by volume deionized water, 1.50% by volume triethanolamine, and 2.00% by volume oleic acid. The bubble size was dependent on the nitrogen flow rate, which we varied using a needle valve. The bubble diameter ranged from 2 to 6 mm, with most bubbles in the 3 to 4 mm range. The resulting bubbles were spooned into a cylindrical Couette viscometer described in detail in Ref. [21]. This produced a two-dimensional wet foam on a homogeneous liquid substrate of 80% by volume deionized water, 15% by volume glycerine, and 5.0% by volume Miracle Bubbles (Imperial Toy Corp.). The Couette viscometer consists of a shallow dish that contains the liquid substrate. Two concentric teflon rings are placed vertically in the dish. The outer ring consists of 12 segmented pieces and has an adjustable radius. The inner ring, or rotor, has a radius $r=4.0$ cm and was suspended by a wire to form a torsion pendulum. Polypropylene balls with a 4 mm diameter were epoxied to the circumference of the inner rotor to prevent the innermost row of bubbles from slipping. The outermost row of bubbles was monitored, and no slip of bubbles on the outer barrier was observed. Figure 1 is a top view of a typical bubble raft in our apparatus. Portions of the two teflon rings are visible.

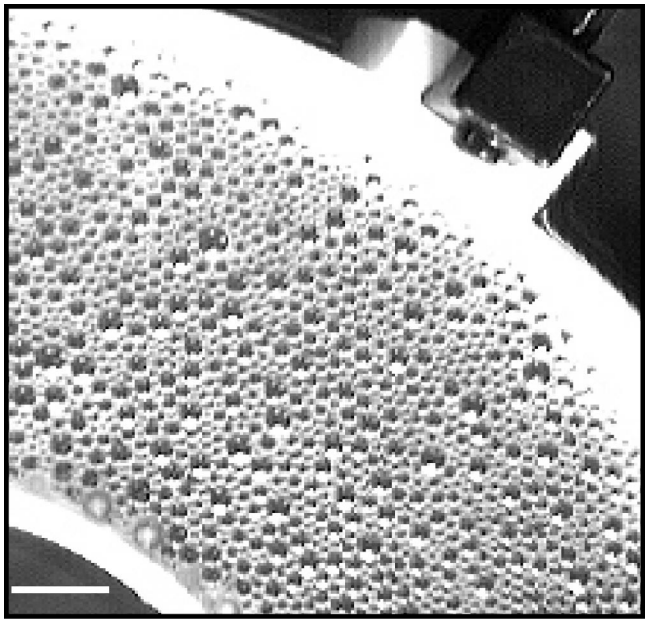

FIG. 1. Image of a section of a typical bubble raft. A portion of the inner rotor is visible in the lower left corner. A portion of the outer barrier is visible in the upper right corner. This particular raft had $\approx 10^4$ bubbles. The scale bar is 1 cm.

To shear the foam, the outer teflon barrier was rotated at a constant angular velocity in the range 0.0005–0.5 rad/s. The torque τ on the inner rotor was monitored by recording the angular position of the inner rotor (and thus the angular displacement of the torsion wire) twice per second. The angular position was measured using magnetic flux techniques described in detail in Ref. [21]. This data was recorded by a 12-bit analog-to-digital converter and stored on a PC. The tangential stress σ on the inner rotor due to the foam is given by $\sigma=\tau/(2\pi r^2)$. During periods without any rearrangements, the fluctuations in the stress were at the level of one bit, corresponding to changes in stress of 2×10^{-3} dyn/cm. Therefore, when computing stress drops, we filtered the data to eliminate any changes in stress of $\pm 2\times10^{-3}$ dyn/cm.

The bubble raft was constructed by placing the approximate number of desired bubbles in the trough with the outer barrier set to a large radius. It is important to note that the bubbles exhibited a strong attraction to each other. This is a microscopic detail that is not included in any of the models discussed in the Introduction. Typically, two-dimensional foams are characterized by their gas-area fraction, which is the ratio of the area filled by gas to the total area. Because the bubbles actually exist in three dimensions for a bubble raft, the fluid walls (and the cross-sectional area of a bubble) are height dependent. This complicates the definition of the

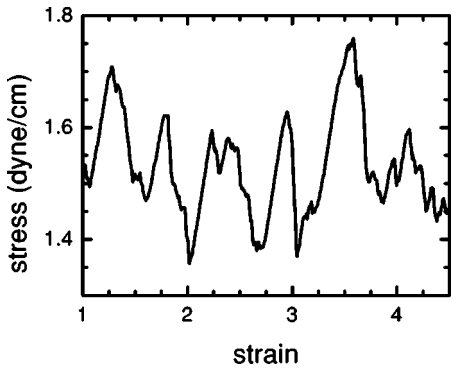

FIG. 2. Typical stress response of a sheared wet foam illustrating the intermittent stress drops. The rate of strain is 0.014 s^{-1} and the number of bubbles is 1.6×10^3.

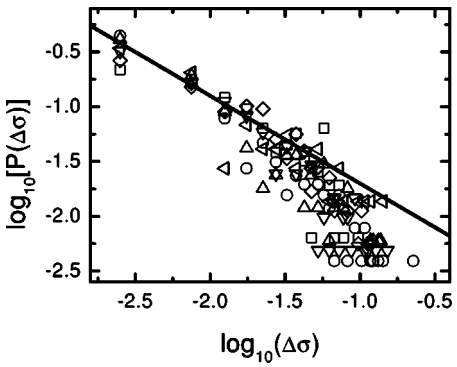

FIG. 3. Probability distribution for stress drops $[P(\Delta\sigma)]$ as a function of the magnitude of the stress drop ($\Delta\sigma\equiv\delta\sigma/\sigma_{max}$). For each separate run, the stress drops $\delta\sigma$ have been normalized by the maximum stress σ_{max}. The symbols represent different strain rates: 2.7×10^{-3} s^{-1} (∇); 1.4×10^{-3} s^{-1} ($\triangle$); 7×10^{-3} s^{-1} ($\triangleleft$); 1.4×10^{-2} s^{-1} ($\bigcirc$); 1.3×10^{-1} s^{-1} ($\diamond$); 2.7×10^{-1} s^{-1} ($\square$). The solid line is a guide to the eye and has a slope of -0.8.

gas-area fraction. Therefore, we used a functional definition for gas-area fraction based on the images of the bubble raft. We defined the area of gas to be the black regions within the bubbles in an image and maintained constant lighting conditions, so that this definition was consistent from run to run. The outer barrier was compressed until the desired bubble density was achieved. It should be noted that this resulted in a variation in the initial shear stress of the bubble raft that did not relax significantly on the time scale of the experiments. Therefore, due to the finite lifetime of the raft, the experiments were carried out with this initial prestress present. Both the total number of bubbles and average gas-area fraction were determined from images of a large section of the trough, assuming an essentially uniform distribution of bubbles throughout the trough. For all the data reported here, the gas-area fraction was ≈0.95.

The stability of the bubbles was enhanced by cooling the fluid substrate to 5 °C. Also, a glass cover was placed over the bubbles. The cover helped to reduce evaporation and was not in contact with the bubbles. The entire apparatus was contained in a cabinet. The cabinet reduced the air flow around the apparatus, and a humidifier placed within the cabinet helped to extend the lifetime of the bubbles. The bubbles in the bubble raft did not exhibit any substantial coarsening with time. Instead, the raft tended to suffer catastrophic failure after ≈2 h due to a significant number of bubbles popping. Presumably, this was due primarily to the loss of fluid in the bubble walls from drainage into the fluid substrate and/or evaporation. Because the bubble raft did not coarsen significantly, there is no competition between coarsening and shear induced rearrangements.

III. EXPERIMENTAL RESULTS

Figure 2 shows the typical behavior of the stress versus strain for strains above the yield strain. The irregular behavior of the stress during flow is apparent. This behavior can be characterized by considering the distribution of stress drops. This is shown in Fig. 3 for a system with 1550 bubbles for various strain rates $\dot{\gamma}$. All results are given in terms of normalized stress drops ($\Delta\sigma\equiv\delta\sigma/\sigma_{max}$), where the stress drops $\delta\sigma$ for each run are normalized by the maximum stress σ_{max} for that run. A bin size for $\Delta\sigma$ of 2.5×10^{-3} was used in plotting the distribution, with the probability of a stress drop of size $\Delta\sigma$ $[P(\Delta\sigma)]$ defined as the number of drops within each bin divided by the total number of drops in the run. The solid line is a guide to the eye and has a slope of -0.8. The distribution is consistent with a power law for small stress drops with an exponential cutoff. Because of the cutoff, there is a well-defined average stress drop, $\langle\Delta\sigma\rangle$. $P(\Delta\sigma)$ for different system sizes are qualitatively the same, a power law for small $\Delta\sigma$, with an exponential cutoff. In order to look for quantitative differences as a function of system size, we considered the behavior of $\langle\Delta\sigma\rangle$.

The average stress drop is shown as a function of strain rate for different system sizes in Fig. 4. The smallest system consisted of 1.6×10^3 bubbles and is given by the squares. For this system, there is essentially no dependence of $\langle\Delta\sigma\rangle$ on strain rate. For the systems with more than 5.6×10^3 bubbles (all of the other systems that we studied), there does appear to be a weak strain rate dependence. One observes an increase in the average stress drop with strain rate, until $\dot{\gamma}\approx0.07$ s^{-1}. Above this value, the average stress drop is in-

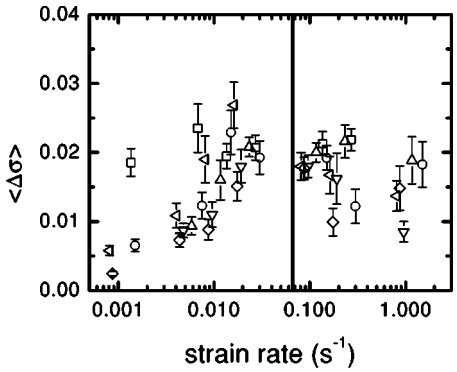

FIG. 4. Plot of the average size of the stress drop ($\langle\Delta\sigma\rangle$) as a function of the strain rate for different system sizes: 1.6×10^3 ($\square$); 5.6×10^3 ($\bigcirc$); 9.2×10^3 ($\triangle$); 1.5×10^4 (∇); 2.0×10^4 ($\diamond$); 2.6×10^4 ($\triangleleft$). The solid vertical line is at $\dot{\gamma}=0.066$ s^{-1}.

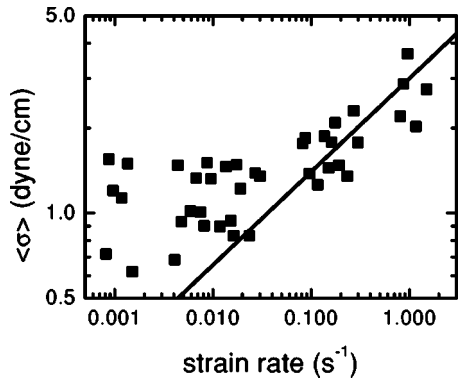

FIG. 5. Plot of the average stress versus the strain rate. The dark line is a guide to the eye, and has slope 1/3.

dependent of strain rate. The implications of this will be discussed in Sec. IV.

One important result is that there is no increase in $\langle \Delta\sigma \rangle$ with system size. This effectively rules out system size as the source of the cutoff. At the lowest strain rates, $\langle \Delta\sigma \rangle$ is lower for the larger systems. A possible reason for this behavior is discussed in Sec. IV.

The relation between average stress and strain rate is shown in Fig. 5. The maximum stress displays a similar dependence. Note the knee of the curve at $\dot{\gamma} \approx 0.07\ \mathrm{s}^{-1}$. A line is drawn as a guide to the eye with a slope of 1/3. The overall curve is consistent with a Herschel-Bulkley model of viscosity, where the stress is given by $\sigma = A + B\dot{\gamma}^n$ [22]. Here, $\dot{\gamma}$ is the strain rate, and A and B are constants. The variation in average stress in Fig. 5 is most likely due to the variation in the initial stress from run to run as discussed in Sec. II. Presumably, if sufficient aging of the system were possible before each run, this variation would be reduced.

An alternate way to view the same data is to consider $\eta \equiv \langle \sigma \rangle / \dot{\gamma}$ versus $\dot{\gamma}$, shown in Fig. 6. This is the steady-state viscosity, taking care to compute $\dot{\gamma}$ at the inner cylinder [22]. The solid line with slope -1 and dashed line with slope $-2/3$ are guides to the eye and clearly illustrate the Herschel-Bulkley behavior of the bubble raft, with an exponent $n = 1/3$. This behavior is consistent with the shear-thinning velocity profile reported in Ref. [5] for $\dot{\gamma} = 0.062\ \mathrm{s}^{-1}$. An open question is the behavior of the velocity profile at extremely low strain rates, where the average stress is essentially independent of strain rate. One definitely observes bubble motions throughout the bulk of the system. However, at these low shear rates, most of the time the system is undergoing a linear increase of the stress, and only occasionally is there a stress drop. Initial measurements of the flow during such an increase in the stress are consistent with a linear profile of the velocity. However, detailed measurements in this regime will be conducted in the future to determine what the long-time average (one that includes many stress drops) of the flow profile is. This is important given the fact that measurements of velocity profiles at low shear rates report an exponential decay of the velocity for a similar system [23]. For our system, one issue is whether or not the water substrate dragged the bubbles. We made a number of measurements where the outer cylinder was rotated, but the bubble raft was not in contact with the outer cylinder. This was accomplished by removing approximately the outer three rows of the bubbles. Under these conditions, no flow of the bubble raft was observed, and no measurable stress was transmitted to the inner rotor. This provides a strong evidence that the underlying water does not "drag" the bubble raft.

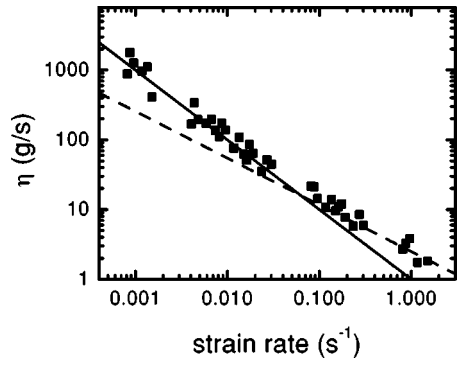

FIG. 6. Plot of the average stress divided by the rate of strain (η) versus the rate of strain. The solid line has a slope of -1 and the dashed line has a slope of $-2/3$. The two lines cross at $\dot{\gamma} = 0.066\ \mathrm{s}^{-1}$.

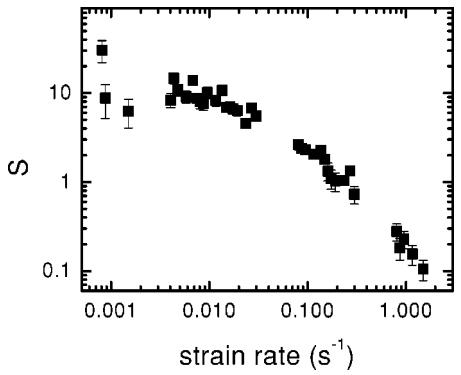

FIG. 7. The number of stress drops per unit strain (S) as a function of strain rate. The plateau at low rates of strain suggests a quasistatic limit is reached.

The dependence of the maximum stress on strain rate suggests the existence of a quasistatic limit. Below a strain rate of $\approx 0.07\ \mathrm{s}^{-1}$, the stress is essentially independent of the rate of strain. This was checked by considering the number of stress drops per unit strain (S). This is plotted in Fig. 7. As with the maximum stress, S approaches a constant below values of the strain rate of $\approx 0.07\ \mathrm{s}^{-1}$.

In addition to the distribution of stress drops, we also characterized the intensity of fluctuations around the mean. We defined the fluctuation intensity Γ as the standard deviation of the stress (after the yield stress) for a given run, expressed as a fraction of the mean stress,

$$\Gamma \equiv \sqrt{\frac{1}{N}\sum_{i=1}^{N}\left(\frac{\sigma_i - \langle\sigma\rangle}{\langle\sigma\rangle}\right)^2}, \qquad (1)$$

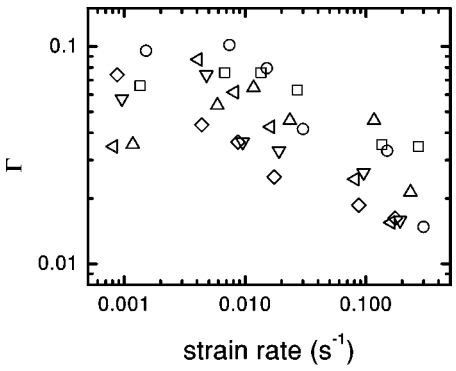

FIG. 8. Fluctuation intensity Γ versus strain rate for a range of system sizes: 1.6×10^3 (□); 5.6×10^3 (○); 9.2×10^3 (△); 1.5×10^4 (▽); 2.0×10^4 (◇); 2.6×10^4 (◁).

where the sum is over the measured values of stress and N is the number of data points for a given experimental run. Given the existence of the prestress, the normalization by the average stress allows for a better comparison between different systems. Figure 8 shows the results for the fluctuation intensity Γ as a function of $\dot{\gamma}$ for the different system sizes. There is significant scatter in the data; however, there is a clear trend of decreasing Γ as $\dot{\gamma}$ increases. One consequence of this is a correlation between Γ and $\langle\sigma\rangle$. This is illustrated in Fig. 9, where the data for the different system sizes are combined into a single plot. Again, there is significant scatter in the data, but the trend is obvious.

IV. SUMMARY

The results presented here provide a strong evidence that the bubble model provides an accurate description of the shear behavior of a bubble raft. To the extent that bubble rafts are equivalent to foam, the bubble model would also describe a two-dimensional flowing foam. The stress drop distribution, the average stress as a function of strain rate (the steady-state viscosity), and the rate of stress drops, S, are all consistent with the bubble model [11]. This agreement is despite the fact that the bubble rafts studied here are strongly attractive, a feature that is not explicit in the model. One interesting result is that both the bubble model and the bubble rafts are well described as a Herschel-Bulkley fluid with an exponent of 1/3 [24]. It remains to be seen if this exponent is a generic feature of the model, and of similar models, or if there is something specific to the parameters used in Ref. [24]. For example, the exponent may depend on various characteristics of the foam, such as the gas-area fraction. This dependence also needs to be tested for the bubble rafts.

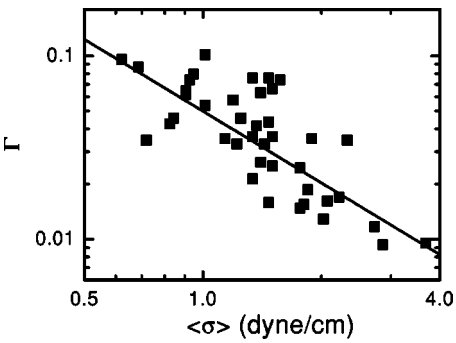

FIG. 9. The fluctuation intensity Γ versus the mean stress. The dark line is a guide to the eye, and has slope -1.3 cm/dyne.

Comparison of our studies with both the quasistatic model [15,16] and the quasistatic experiments [20] raises an interesting question: is there a fundamental difference between slow but steady shear and true quasistatic motions? The disagreement between our results and the quasistatic experiments suggests that such a difference may exist. However, it is also possible that the discrepancies are due to comparing direct measurements of the stress drops with sizes of spatial rearrangements. Future work with our system will look at both the issue of quasistatic steps versus steady shear and the spatial extent of rearrangements.

With regard to the extended q-Potts model, this work raises some important questions. Two clear predictions of this model are (1) there is no quasistatic limit; and (2) a sufficiently disordered foam no longer has a yield strain [17]. Neither behavior was observed in our experiments. At this point, one would need to do further work to determine if there was something fundamentally missing from the q-Potts model that results in this disagreement. The other possibility is that our foams were either not sufficiently disordered to be accurately described by the q-Potts model or they were not sufficiently dry, as the simulations in Ref. [17] were for dry foam. Therefore, future experiments will focus on the role of disorder and the wetness of the foam.

Though not conclusive, the behavior of the average stress drop as a function of system size and strain rate, shown in Fig. 4, suggests some interesting behavior. The large decrease in $\langle\Delta\sigma\rangle$ as a function of system size is surprising. One possible explanation involves the spatial correlations between bubble rearrangements that produce the stress drops. As the system size increases, there are more spatial locations at which rearrangements can occur. For low enough strain rates, there will be an intermediate range of systems size for which this increases the probability of isolated small stress drops occurring. Once one region slips, enough stress is relieved such that the other regions do not rearrange until a sufficiently later time that they are recorded as a new stress drop. Such dynamics would result in a decrease in the average stress drop with system size. Eventually, as the system size increases even more, this behavior should ''smooth'' out the dynamics, as small stress drops occur almost continuously. Presumably, this happens in large, three-dimensional samples. On the other hand, for these intermediate size systems, as the strain rate is increased, the stress releases occur closer together. This increases the likelihood of multiple small events in different spatial locations combining to form larger stress drops. Therefore, one observes an increase in the average stress drop as a function of strain rate. Eventually, as the system crosses over to more fluidlike behavior, there is again a smoothing of the dynamics. In this regime, the average stress drop becomes independent of the strain rate. Clearly, more work is needed, both in experiments and simulations, to test these ideas. In particular, they highlight the

importance of measuring both spatial correlations between rearrangement events and the correlation between the rearrangements and the stress drops.

Finally, it interesting that the crossover to smoother, more fluidlike behavior, as a function of strain rate, is evident in both the measurement of Γ and $\langle \Delta\sigma \rangle$. However, the two measures reveal a slightly different behavior. As one increases the strain rate, Γ decreases monotonically (see Fig. 8). However, $\langle \Delta\sigma \rangle$ becomes independent of $\dot{\gamma}$ at the higher strain rates (see Fig. 4). The two results are not inconsistent, since Γ measures the size of fluctuations from the mean, while $\langle \Delta\sigma \rangle$ measures the average size of the changes in stress that produce these fluctuations. Again, understanding the spatial distribution of bubble rearrangements will probably be an important step in fully understanding the dependence of these two measures of the fluctuations on strain rate.

ACKNOWLEDGMENTS

The authors acknowledge funding from NSF Grant No. CTS-0085751. M.D. acknowledges further funding from the Research Corporation and Alfred P. Sloan Foundation. E.P. was supported by NSF Research Experience for Undergraduates (REU) Grant No. PHY-9988066. The authors thank A. J. Liu and C. O'Hern for useful discussion on the bubble model and Y. Jiang for discussion on the *q*-Potts model.

[1] I.K. Ono, C.S. O'Hern, D.J. Durian, S.A. Langer, A.J. Liu, and S.R. Nagel, Phys. Rev. Lett. **89**, 095703 (2002).
[2] L. Berthier and J.-L. Barrat, Phys. Rev. Lett. **89**, 095702 (2002).
[3] *Jamming and Rheology*, edited by A.J. Liu and S.R. Nagel (Taylor & Francis, London, 2001).
[4] A.S. Argon and H.Y. Kuo, Mater. Sci. Eng. **39**, 101 (1979).
[5] J. Lauridsen, M. Twardos, and M. Dennin, Phys. Rev. Lett. **89**, 098303 (2002).
[6] A.M. Kraynik, Annu. Rev. Fluid Mech. **20**, 325 (1988).
[7] J. Stavans, Rep. Prog. Phys. **56**, 733 (1993).
[8] D. Weaire and S. Hutzler, *The Physics of Foams* (Clarendon Press, Oxford, 1999).
[9] D.J. Durian, Phys. Rev. Lett. **75**, 4780 (1995).
[10] D.J. Durian, Phys. Rev. E **55**, 1739 (1997).
[11] S. Tewari, D. Schiemann, D.J. Durian, C.M. Knobler, S.A. Langer, and A.J. Liu, Phys. Rev. E **60**, 4385 (1999).
[12] K. Kawasaki, T. Nagai, and K. Nakashima, Philos. Mag. B **60**, 399 (1989).
[13] T. Okuzono and K. Kawasaki, Phys. Rev. E **51**, 1246 (1995).
[14] K. Kawasaki, T. Okuzono, T. Kawakatsu, and T. Nagai, in *Proceedings of the International Workshop of Physics of Pattern Formation*, edited by S. Kai (World Scientific, Singapore, 1992).
[15] D. Weaire, F. Bolton, T. Herdtle, and H. Aref, Philos. Mag. Lett. **66**, 293 (1992).
[16] S. Hutzler, D. Weaire, and F. Bolton, Philos. Mag. B **71**, 277 (1995).
[17] Y. Jiang, P.J. Swart, A. Saxena, M. Asipauskas, and J.A. Glazier, Phys. Rev. E **59**, 5819 (1999).
[18] A.D. Gopal and D.J. Durian, Phys. Rev. Lett. **75**, 2610 (1995).
[19] M. Dennin and C.M. Knobler, Phys. Rev. Lett. **78**, 2485 (1997).
[20] A.A. Kader and J.C. Earnshaw, Phys. Rev. Lett. **82**, 2610 (1999).
[21] R.S. Ghaskadvi and M. Dennin, Rev. Sci. Instrum. **69**, 3568 (1998).
[22] R.B. Bird, R.C. Armstrong, and O. Hassuage, *Dynamics of Polymer Liquids* (Wiley, New York, 1977).
[23] G. Debrégeas, H. Tabuteau, and J.M. di Meglio, Phys. Rev. Lett. **87**, 178305 (2001).
[24] S.A. Langer and A.J. Liu, Europhys. Lett. **49**, 68 (2000).